VARIOUS RESPONSE FUNCTIONS IN LATTICE DOMES RELIABILITY VIA ANALYTICAL INTEGRATION AND FINITE ELEMENT METHOD

B. POKUSIŃSKI and M. KAMIŃSKI[*]
Chair of Structural Reliability
Faculty of Civil Engineering Architecture and Environmental Engineering
Łódź University of Technology
Al. Politechniki 6, 90-924 Łódź, POLAND
E-mail: marcin.kaminski@p.lodz.pl

The main aim of this work is to verify an influence of the response function type in direct symbolic derivation of the probabilistic moments and coefficients of the structural state variables of axisymmetric spherical steel dome structures. The second purpose is to compare four various types of domes (ribbed, Schwedler, geodesic as well as diamatic) in the context of time-independent reliability assessment in the presence of an uncertainty in the structural steel Young modulus. We have considered various analytical response functions to approximate fundamental eigenfrequencies, critical load multiplier, global extreme vertical and horizontal displacements as well as local deformations. Particular values of the reliability indices calculated here can be of further assistance in the reliability assessment by comparing the minimal one with its counterpart given in the Eurocode depending upon the durability class, reference period and the given limit state type.

Key words: response function method, semi-analytical probabilistic technique, lattice dome structures, reliability analysis, weighted least squares method.

1. Introduction

Domes are one of the oldest and well-established structural forms and have been used in architecture since the earliest times (Lan, [1]). However, their lattice versions have begun to be constructed in the 19th century, when the steel and cast iron production technology was developed (Szaniec and Biernacka, [2]). Since then, they have been of special interest to structure designers as they enclose a maximum amount of space with a minimum surface and have proved to have very economical strength-to-weight ratios (Lan, [1]). Therefore, it seems essential to examine their reliability and additionally compare it for several selected types frequently used in practice. Computer analysis of civil engineering structures with random parameters has a remarkably increasing influence on structural design processes, optimization and reliability modelling because of a variety of natural sources of uncertainties and human activity driven reasons. In the case of the domes examined, the Young modulus uncertainty, as one of the most important parameters, has been considered. A solution of the structural problem including randomness is accompanied with the reliability indices verification, according to the general rules included in the Eurocode [3]. Their determination has been provided here by an application of the global version of the response function method and the direct symbolic integral calculation of its basic probabilistic moments. Computational implementation of this method has been made for a solution of the eigenproblem, stability and static problems using the FEM civil engineering system ROBOT. The integration process has been provided by the computer algebra system MAPLE, where also the coefficients of responses have been computed from several solutions of the original problem obtained for the Young modulus varying about its expectation. This form leads to a determination of all structural response functions with respect to the random Gaussian input variable. They can be further used for the determination of probabilistic moments and final values of the reliability indices. Finally, the results may be compared to find out which structure is more efficient in terms of the assumed uncertainty.

---

* To whom correspondence should be addressed

However, the main aim of this work is to verify the influence of the response functions choice on the probabilistic moments and coefficients. This problem has been examined in the perturbation method (Pokusiński and Kamiński, [4]), but it is not known how much the method itself influenced the results. Here, the direct symbolic integration approach has been used which is the most accurate method. Once the response function represents a direct dependence, we obtain a solution of the analytical method (AM), but when it is only an initial approximation – of the semi-analytical method (SAM). Therefore, we have considered performance functions concerning the basic eigenfrequency, the critical coefficient, the global extreme vertical and horizontal displacements as well as local deformation. They have a well-known form of analytical dependence and can be used to examine their various approximations. In the first part of the analysis, rational functions and polynomials have been tested. Then, generalizations of the most frequently used empirical formulas have been employed.

The influence of the analyzed response functions on the results has been compared numerically. The maximum value of the input coefficient of variation has been sought for which the SAM results would be close to those obtained from the reference analytical method. Attempts have also been made to find dependences of the above value on some criterion value of the FEM experiments series with the proposed approximation. The final goal was to find a limit value of such a criterion, above which a satisfactory correctness is achieved – to use it when a structural response is unavailable. In most practical cases this situation is very frequent, which is a fundamental problem in the reliability analysis.

In the first part of the analysis, the influence of the trial points number has been analyzed also. It involves changing the width of the considered interval in the response function method. If it is narrow (Kamiński and Szafran, [5]; Solecka *et al.*, [6]), there is a risk that the results may not adequately indicate the complexity of the function. In addition, the method actually provides an approximation primarily within the interval. However, in the case of the direct integration approach, the integration values are in a much wider range.

2. Direct symbolic integration approach

In the case of some real function $f(b)$ of the stationary input random variable b with its probability density function as $p_b(x)$, classical definitions of some probabilistic moments and coefficients are as follows (Kamiński, [7]; Kottegoda and Rosso, [8]; Murzewski, [9]):
  −   the expectation

$$E\big[f(b)\big] = \int_{-\infty}^{+\infty} f(b) \cdot p_b(x) dx, \tag{2.1}$$

  −   the variance

$$\mathrm{Var}\big(f(b)\big) = \int_{-\infty}^{+\infty} \big(f(b) - E\big[f(b)\big]\big)^2 \cdot p_b(x) dx, \tag{2.2}$$

  −   the *m*th central probabilistic moment (for *m > 2*)

$$\mu_m\big(f(b)\big) = \int_{-\infty}^{+\infty} \big(f(b) - E\big[f(b)\big]\big)^m \cdot p_b(x) dx, \tag{2.3}$$

  −   the coefficient of variation

$$\alpha\big(f(b)\big) = \frac{\sqrt{\mathrm{Var}\big(f(b)\big)}}{E\big[f(b)\big]}, \tag{2.4}$$

– the skewness

$$\beta_s\left(f(b)\right)=\frac{\mu_3\left(f(b)\right)}{\left(\sqrt{\mathrm{Var}\left(f(b)\right)}\right)^3}, \tag{2.5}$$

– and the kurtosis

$$\kappa\left(f(b)\right)=\frac{\mu_4\left(f(b)\right)}{\left(\mathrm{Var}\left(f(b)\right)\right)^2}-3. \tag{2.6}$$

The Gaussian probability density function has been considered, so that

$$p_b(x)=\frac{1}{\sigma(b)\cdot\sqrt{2\cdot\pi}}\exp\left\{-\frac{\left(x-E[b]\right)^2}{2\cdot\sigma^2(b)}\right\}\qquad\left(x\in\Re\right) \tag{2.7}$$

where $\sigma(b)$ stands for the standard deviation of the input random variable substituted further by a product of the expected value $E[b]=b^0$ and input coefficient of variation α.

From the numerical point of view, the integral definitions – Eqs (2.1)-(2.3). – are very rarely used with infinite limits. Random variables usually are analyzed as truncated with lower and upper bounds driven by physical meaning of the specific parameter, or just the experimental works. Here, the integration process is limited using the three-sigma rule. Once the function $f(b)$ represents a direct dependence, we obtain a solution of the analytical method (AM), but when it is only an initial approximation – of the semi-analytical method (SAM). It is worth emphasizing that in most practical cases, this structural response is unavailable.

3. Response function method

As shown above, one of the crucial issues during applying the symbolic integration is numerical determination of the structural response function with respect to the randomized parameter. To complete this task, it is necessary to determine such a function by a multiple solution of the boundary value problem about the mean value of the random parameter, in the interval $\left[b^0-\Delta b, b^0+\Delta b\right]$. There are several ways to choose the $\Delta b/b^0$ ratio as well as this interval subdivision both in terms of uniformity and the number of trial points (Kamiński and Szafran, [10]; Kamiński and Świta, [11]; [12]). In the first part of the analysis, an influence of some various configurations (Tab.1) on the final results has been examined.

Table 1. Trial points for their given number.

N	E[b]x																
	0.10	0.50	0.60	0.70	0.80	0.90	0.95	0.96	...	1.04	1.05	1.10	1.20	1.30	1.40	1.50	1.90
11							+	+	+	+	+						
13						+	+	+	+	+	+	+					
15					+	+	+	+	+	+	+	+	+				
17				+	+	+	+	+	+	+	+	+	+	+			
19			+	+	+	+	+	+	+	+	+	+	+	+	+		
21		+	+	+	+	+	+	+	+	+	+	+	+	+	+	+	
23	+	+	+	+	+	+	+	+	+	+	+	+	+	+	+	+	+

Each unknown response function has been approximated here by rational functions $u(b)/v(b)$ computed using the Rational Interpolation (Beckermann and Labahn, [13]; [14]). The Least Squares Method, as well as its weighted version (WLSM), have also been used to obtain commonly applied polynomial responses $w(b)$ (Kamiński and Szafran, [10]; Kamiński and Świta, [11]; [12]). In the latter method, the values computed for the expectation of the Young modulus (*210* GPa) have been recognized as crucial. Their weights (*10*) have been assumed as the sum of the rest ten weights of equivalent results (equals *1*).

Table 2. Groups of functions for the LSM and $N = 11$.

Group name	Function number	Formula
F0	1-10	$w(b)$
F1	1-10	$e^{w(b)}$
F2	1-10	$\sqrt{w(b)}$
F3	1-10	$\dfrac{1}{w(b)}$
F4	1-10	$\dfrac{b}{w(b)}$
F5	1-10	$w(1/b)$
F6	1	$C \cdot b^D$
	2	$C \cdot D^{\frac{1}{b}}$
	3	$C \cdot \ln(b) + D$
	4	$\sqrt{C \cdot \ln(b) + D}$
	5	$\dfrac{1}{C \cdot \ln(b) + D}$
	6	$\dfrac{b}{C \cdot \ln(b) + D}$
	7	$\dfrac{1}{\dfrac{C}{b} + D}$
	8	$\dfrac{b}{\dfrac{C}{b} + D}$

The following polynomial orders have been considered: from *1* to *10* for $w(b)$, from *0* to *10* for $v(b)$ and from *0* to the maximum possible (dependent on the trial points number N, but not more than *10*) for $u(b)$. However, the rational functions having vertical asymptotes in the integration interval have been omitted (actual functions do not have such anomalies).

In the second part of the analysis, generalizations of the most frequently used empirical formulas (Bronsztejn *et al.*, [15]) have been used (Tab.2) if possible. Several proposed functions (group F6) obtained in the rectification procedure have also been verified.

The well-known analytical dependences for elastic displacements, the critical coefficient and the first eigenfrequency have been assumed as reference response functions

$$f(b) = \frac{C}{b}, \tag{3.1}$$

$$f(b) = C \cdot b, \tag{3.2}$$

$$f(b) = C \cdot \sqrt{b}. \tag{3.3}$$

The criteria of maximizing correlation (*K*), minimizing variance (*V*) and maximizing their quotient (*M*) have been used to find the optimal function. Mixed criteria have also been created for least-squares based approximations because the analytical dependences have later turn out to be hardly sensitive to the weights distributions. The criterion K1 assumes, for example, the product of the correlation between the LSM and the WLSM solution with the first power of the correlation of the FEM experiments series with the proposed fitting. The criteria V1, M1, K2, V2 and M2 have been obtained analogously. The minimum from all models is hereinafter called the criterion value so that the given response function type would describe all the different domes equally well.

4. Finite element analysis

All the numerical experiments contained in this work have been carried out with the use of the FEM system ROBOT, where the BFGS algorithm for P-delta analysis is implemented. Its usage was driven by the fact that this system enables both the structural FEM analysis as well as shaping and dimensioning of steel structures, so that reliability analysis is fully supported by this program and enables (1) in particular full variations of the steel connection stiffnesses – from a hinge up to the full restrain, (2) computer analysis of the beams with linear variations of their webs. The following parameters have been set to complete these experiments:

- a number of the load increments equals 5,
- maximum number of iterations per an increment equals 40,
- a number of reductions for the increment length equals 3,
- a coefficient of the increment length reduction – 0.5,
- a control parameter of the line search method – 0.5,
- maximum number of the BFGS corrections – 10,
- a tolerance factor of the relative norm for the residual forces – 0.0001,
- a tolerance factor for the relative norm of displacements – 0.0001.

It should be mentioned also that all structural matrices and vectors have been updated after each sub-increment.

All these numerical tests have been performed on the four types of the domes: ribbed (Model R), Schwedler (Model S), geodesic (Model G) and diamatic (Model D), presented correspondingly in Figs 1-4. These are computational models of the supporting steel structure for the hemisphere glass roof with the radius of *20.0 m*. Model R (Fig.1) is constructed by mutually perpendicular *36* meridians and *17* rings. Their positions result in the formation of *612* panels in the shape of trapeziums whose legs have the same length as longer bases. Top ring has the diameter of *4.92 m*. Model S (Fig.2) has been created by adding one diagonal in every trapezoidal panel of Model R. Model G (Fig.3) is *8* frequency class-*I* geodesic dome made on the base of icosahedron (then the differences between lengths of members are the smallest). It is crowned with a regular pentagon with the side length of *2.80 m*. Finally, Model D (Fig.4) is based on a sixth of the hemisphere with equal division of meridians (into *10* parts) and rings (divided into more and more parts starting from one for the top). The side length of the crown hexagon equals *3.13 m* and the trusses are resultant.
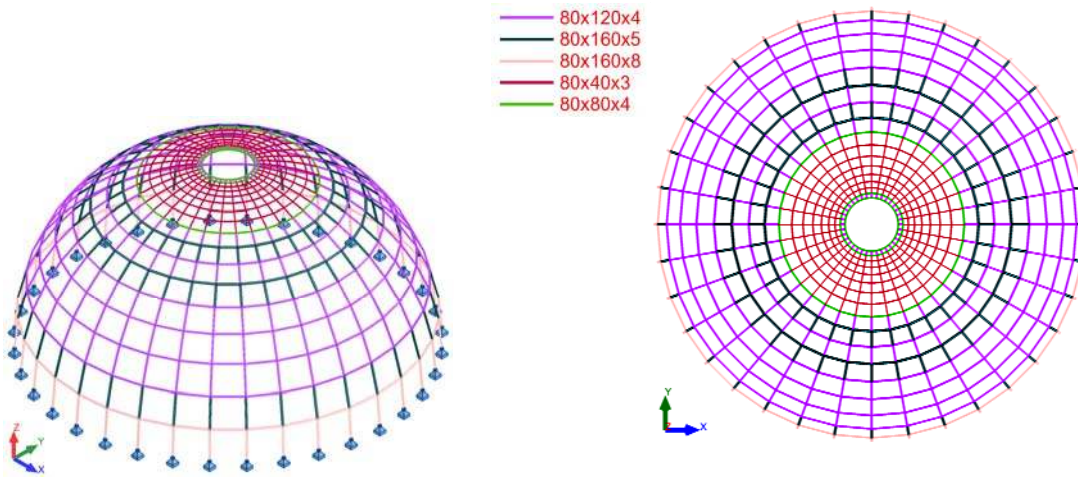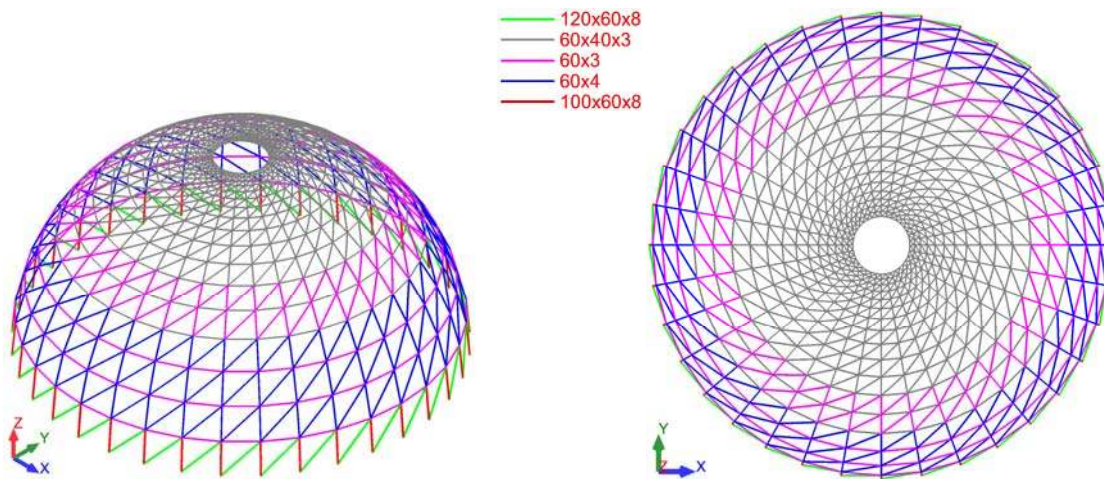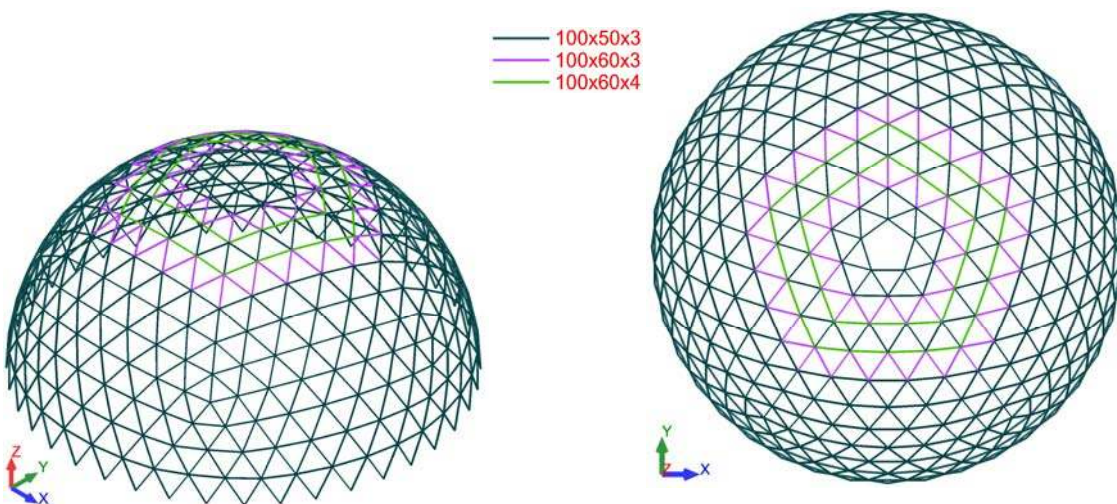
Fig.1. Model R.

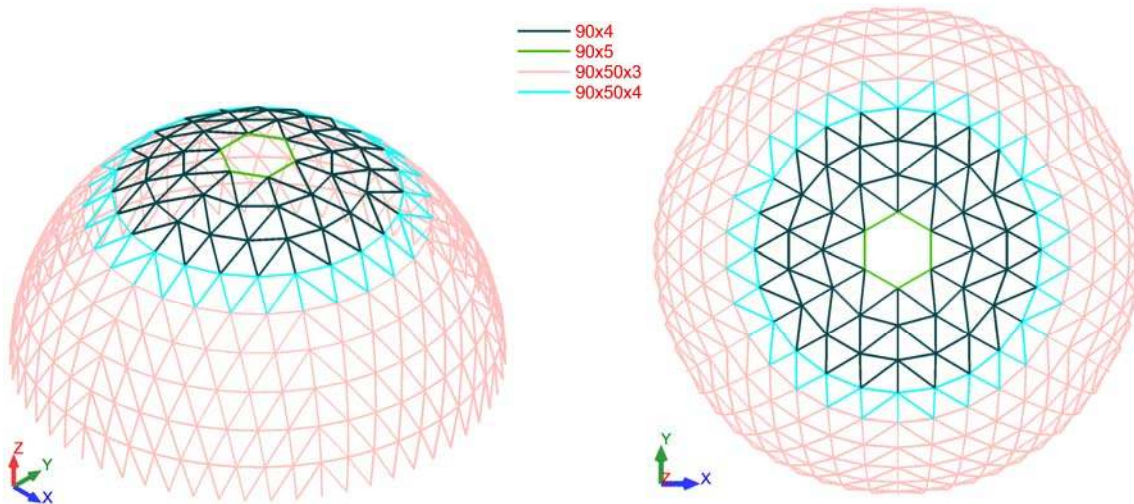Fig.2. Model S.

Fig.3. Model G.

Fig.4. Model D.

The 3D frame two-noded finite elements with 6 degrees of freedom in each node and rigid connection have been used in each model. All of the supports have been defined as rigid with fixed movements and free rotations in each direction. They rest on the ground level. Table 3 shows the properties of the models in detail.

Table 3. Properties of the models.

Model	Nodal points	Supports	Bars	Minimal bar length [m]	Maximal bar length [m]	Groups of bars of the same length	Panels	Weight [kg]
R	648	36	1224	0.43	3.43	30	612	28 574
S	648	36	1836	0.43	4.88	50	1224	21 670
G	350	40	935	2.39	3.29	33	635	19 446
D	330	60	864	2.30	4.14	57	594	20 244

The number of nodes and structural members is much larger in the first two models. However, for the supports the situation is contrary, with the exception of Model G, where the difference is smaller. The length of structural members is both the result of the type of dome as well as fulfilment of the maximum dimension condition of glass panels. The smallest differences are for Model G, a little bigger for Model D, much bigger for Model R and the biggest for Model S. However, for Model R and G the groups number of the same length bars is much smaller than for the rest. The geodesic dome has minimal weight and the ribbed one – clearly the biggest.

All loads from Eurocode 0 [3] have been considered for the 50 years design working life (common structure). The first (permanent loads – Gp, Fig.5a) is connected with the weight of the toughened glass covering (*2.4 cm* thick layer) and supporting structure itself. The next two represents snow loads for the second zone in Poland according to Eurocode 1-1-3 [16] for undrifted (Sud, Fig.5b) and drifted (Sd, Fig.5c) arrangements. The rest three cases are connected with wind actions from Eurocode 1-1-4 [17] for the first zone in Poland (terrain category III) caused by negative internal pressure (Win, Fig.5d), positive internal pressure (Wip, Fig.5e) and external pressure (We, Fig.5f). A few wind directions (and corresponding drifted snow loads) have been considered due to the different orientation of the models symmetry planes (Figs 6a-d). Imposed live loads have not been defined because for a roof of category H (not accessible except for normal maintenance and repair according to Eurocode 1-1-1 [18]), the factor for combination value equals 0 (Eurocode 0, [3]).
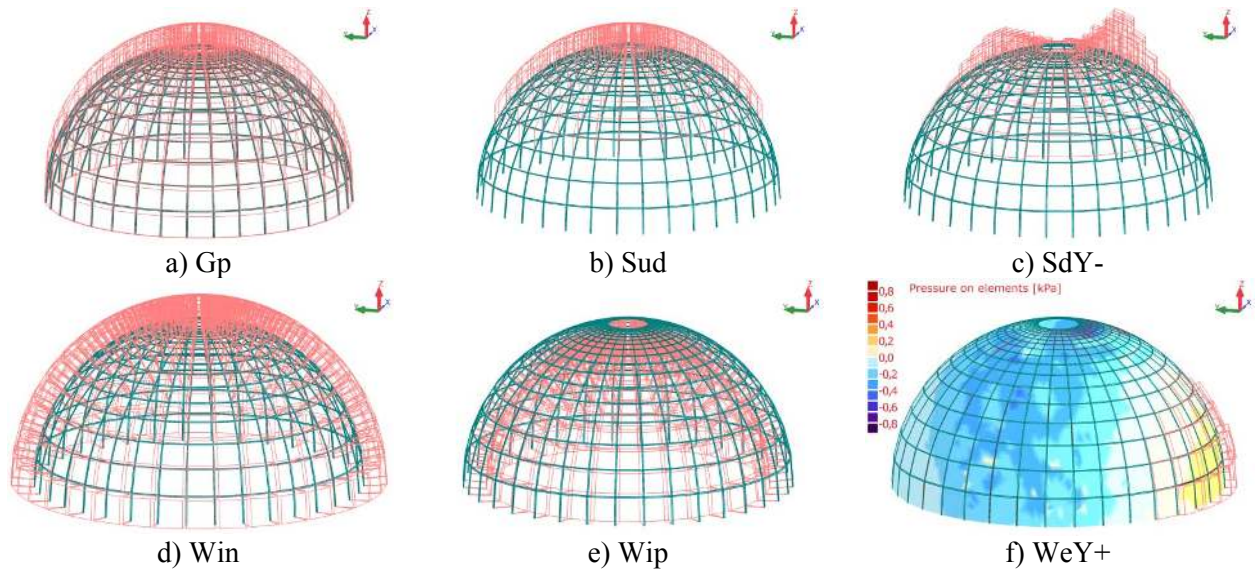
| a) Gp | b) Sud | c) SdY- |
| d) Win | e) Wip | f) WeY+ |

Fig.5. Some load cases implementations on the example of Model R.

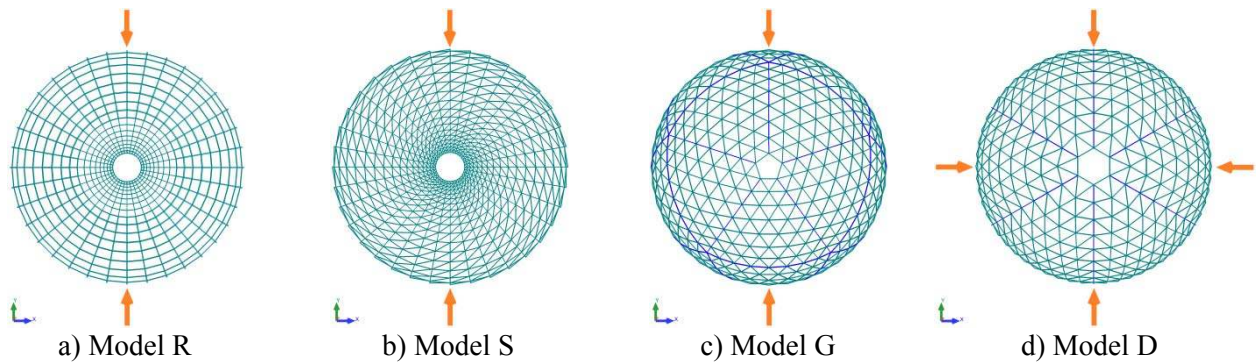| a) Model R | b) Model S | c) Model G | d) Model D |

Fig.6. Different wind directions.

The Serviceability Limit State (SLS, Fig.7) and the Ultimate Limit State (ULS) have been considered by using first-order elastic analysis as well as second-order global analysis P-Delta to more realistically predict the structural behavior (Eurocode 3-1-1, [19]). The incremental method (5 increments) with updating the matrix after each subdivision has been used to solve the second problem. Table 4 shows the considered types of combinations (Eurocode 0, [3]).

Table 4. Types of combinations (S*=Sud or Sd for some wind direction, We*=We for some wind direction).

Type of combination	ULS	SLS
1	$1.35 \cdot 0.85 \cdot \mathrm{Gp} + 1.5 \cdot \mathrm{S}^* + (1.5 \cdot 0.6 \cdot \mathrm{We}^* + 1.5 \cdot 0.6 \cdot \mathrm{Win})$	$\mathrm{Gp}+\mathrm{S}^*+(0.6 \cdot \mathrm{We}^* + 0.6 \cdot \mathrm{Win})$
2	$1.35 \cdot 0.85 \cdot \mathrm{Gp} + 1.5 \cdot \mathrm{We}^* + 1.5 \cdot \mathrm{Win} + (1.5 \cdot 0.5 \cdot \mathrm{S}^*)$	$\mathrm{Gp}+\mathrm{We}^*+\mathrm{Win}+(0.5 \cdot \mathrm{S}^*)$
3	$1.0 \cdot \mathrm{Gp} + 1.5 \cdot \mathrm{We}^* + 1.5 \cdot \mathrm{Wip}$	$\mathrm{Gp}+\mathrm{We}^*+\mathrm{Wip}$

The occurrence of elements that perform the function of bracings has a significant influence on the shape and size of the deformation of the structure (Fig.7). The ribbed dome (without such elements) is characterized by significantly bigger differences between the results of the first and second order analysis as well as in the deformation itself (over 3 times larger maximum vertical deflection and more than 10 times greater global horizontal displacement from the rest). This is one of the reasons why Model D clearly has the maximum weight (Tab.3).

The Finite Element Method based modal analysis and linear elastic buckling analysis have been performed, too. Higher modes have also been computed, but only a verification of the first mode has been performed. The

subspace iteration algorithm has been used for solving these problems. In the first buckling mode of Model S, G and D (Figs 8b-d) a few elements have much larger deformation than the rest (member or local buckling). This is caused by differences in the ratio distribution of the compressive force to the critical force. In Model R overall buckling of the whole structure occurs (Fig.8a). Local buckling rather plays the role of a trigger here.

Yield strength has been assumed as *235* MPa and the structural members have been made of rectangular hollow sections (Tab.5, Figs 1-4). This type of cross-section has been chosen because of its insensitivity to the lateral-torsional buckling and hence it is usually used in structures with glass covers.

a) Model R (scale 50x)   b) Model S (scale 100x)

c) Model G (scale 200x)   d) Model D (scale 200x)

Fig.7. Deformation of the structures.

a) Model R (scale 1500x)   b) Model S (scale 750x)

c) Model G (scale 500x)   d) Model D (scale 300x)
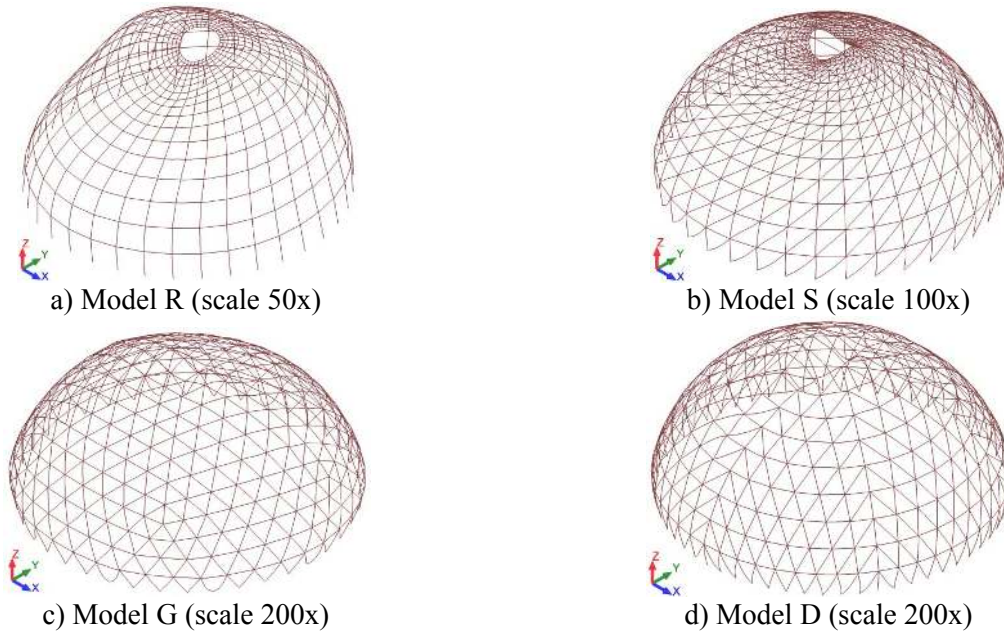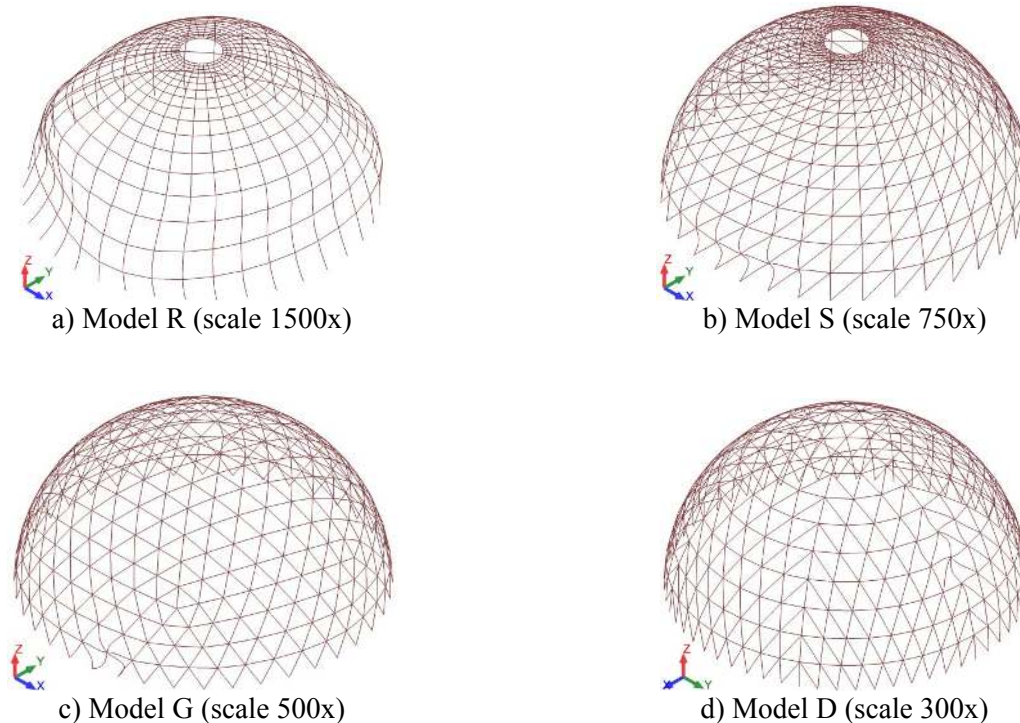
Fig.8. The first buckling mode (for ULS combinations).

Table 5. Number of elements with a specific cross-section.

No.	Model R		Model S		Model G		Model D	
	Section RHS	Number of bars/groups of the same length	Section RHS	Number of bars/groups of the same length	Section RHS	Number of bars/groups of the same length	Section RHS	Number of bars/groups of the same length
1	*80x40x3*	*468/13*	*60x40x3*	*1296/35*	*100x50x3*	*830/21*	*90x50x3*	*660/41*
2	*80x80x4*	*108/3*	*60x60x3*	*252/7*	*100x60x3*	*70/8*	*90x50x4*	*78/6*
3	*80x120x4*	*396/9*	*60x60x4*	*216/6*	*100x60x4*	*35/4*	*90x90x4*	*120/9*
4	*80x160x5*	*180/4*	*60x100x3*	*36/1*	-	-	*90x90x5*	*6/1*
5	*80x160x8*	*72/1*	*60x120x8*	*36/1*	-	-	-	-

In each model the sizing process was similar and deterministic: carried out according to Eurocode 3-1-1 [19]. Initially, an identical RHS section was adopted for all bars of a given dimension in the normal direction. Next, division into groups of bars was made taking into account the distribution of internal forces in ULS combinations and deformations in SLS combinations (Fig.7). For each of them, a cross-section with a given dimension in the normal direction was calculated. In the first phase, the results of the first order analysis were taken into account and the local deformations SLS condition and ULS conditions were verified with the assumption of $\mu = 0.75$ (*1.0* for Model R). Then, all SLS and ULS conditions were checked for the results of the P-Delta analysis. In the last stage, ULS conditions for real μ were verified, which were obtained from the buckling analysis of bars with a given cross-section. The process of creating groups and sizing their cross-sections was iterative. Its limitations were: the given dimension of RHS in the normal direction and the use of up to 5 available profiles in the structure. The above procedure was carried out for various constant dimensions in the normal direction, finally choosing one for which the lowest mass was obtained. As a result, the approximate weight of Model R (counted based on the lengths of model members, not the real structural elements) has reached *28 574 kg*, Model S – 21 670, Model D – 20 244, when Model G only *19 446 kg* (Tab.3). The number of bars with a specific cross-section is given in Tab.5.

The purpose of computational analysis is to determine, for all examples of the structures, the fundamental frequency, the minimal critical coefficient, the extreme horizontal displacement, the maximum of the global vertical deflection and local deformation of the domes members. The reduced stresses have not been considered because the Young modulus does not influence their results as the stiffness proportions remain stable.

5. Computational reliability analysis

For all examples of the structures, each previously mentioned response has been adopted to approximate its dependence on the randomized Young modulus. The probabilistic moments and coefficients have been computed by using Eqs (2.1)-(2.7) and some reference results are shown in Figs 9-13.

The expectations results for analytical dependences (Fig.9.) coincide with an engineering intuition in this matter. For the variance (Fig.10), there are still some differences between the models, but starting from the coefficient of variation the results (Figs 11-13) are already identical. The responses are proportional, so the distributions of the probability density functions for the given parameter do not differ in shape at all but only in the location of their symmetry axes. It is worth emphasizing that the resulting coefficient of variation for the horizontal displacements, local and global deflections (Figs 11a-c) is linearly dependent upon the input one in the interval $\alpha \in [0.0, 0.10]$, while for larger values the increase of the final value is more and more rapid. When the coefficient of variation of the fundamental frequency is concerned (Fig.11e), the dependence is almost linear with the slope close to one half. It equals, of course, one for the critical coefficient (Fig.11d).
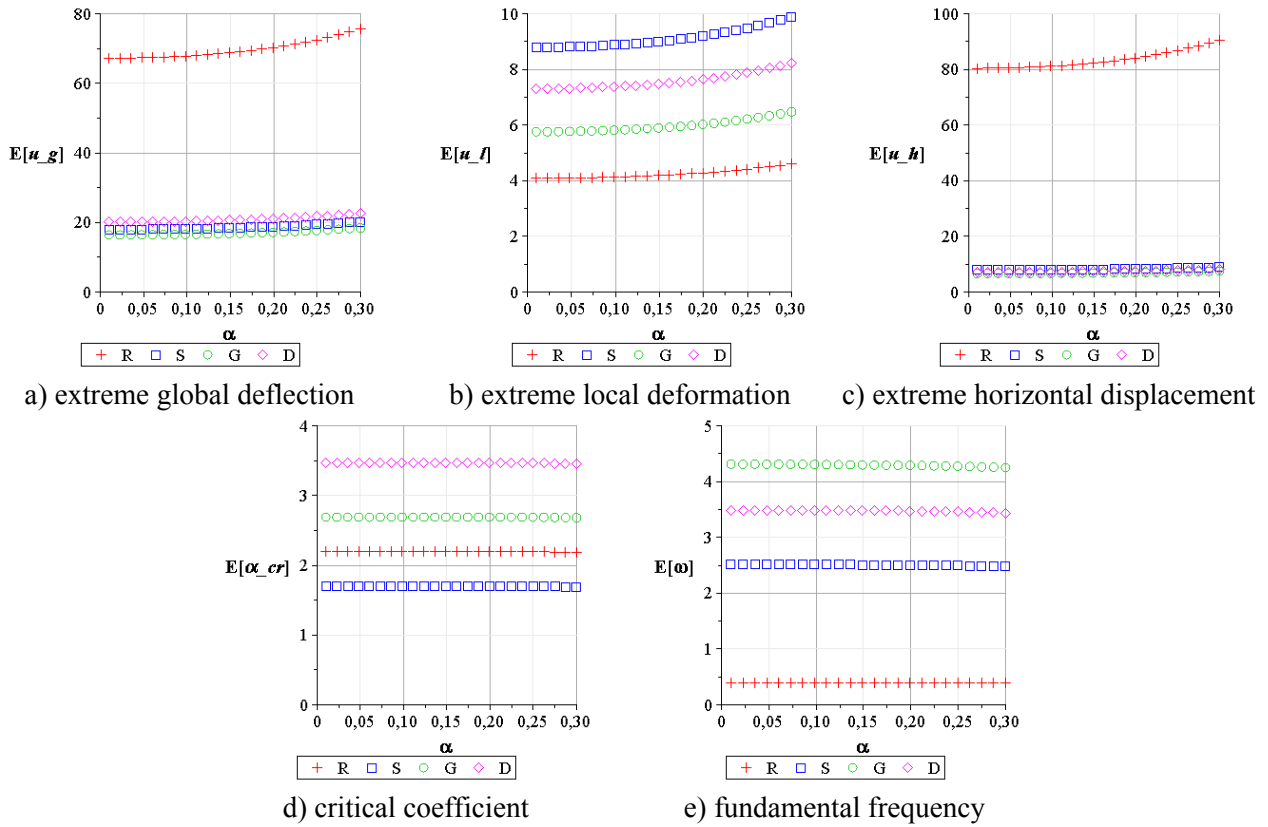
a) extreme global deflection   b) extreme local deformation   c) extreme horizontal displacement

d) critical coefficient   e) fundamental frequency

Fig.9. Expected values for the analytical dependences.

a) extreme global deflection   b) extreme local deformation   c) extreme horizontal displacement

d) critical coefficient   e) fundamental frequency
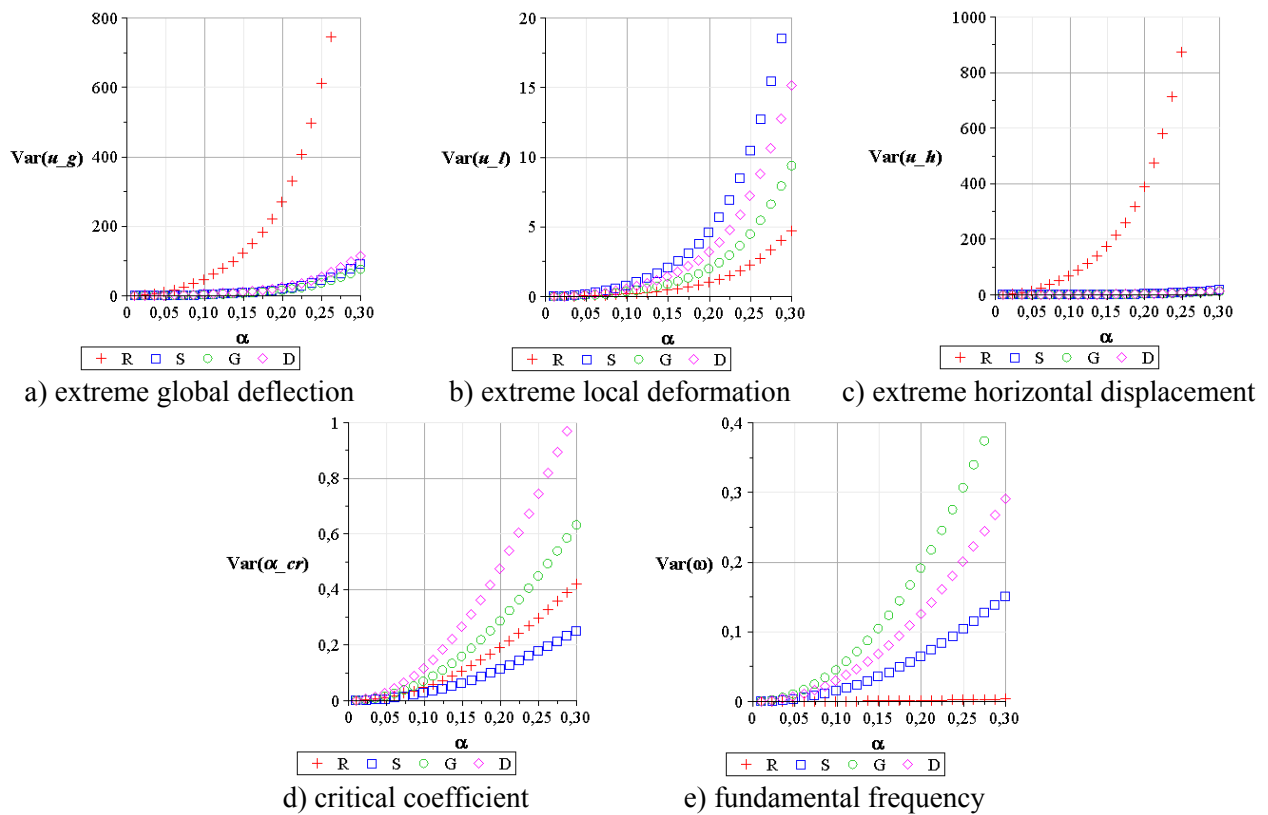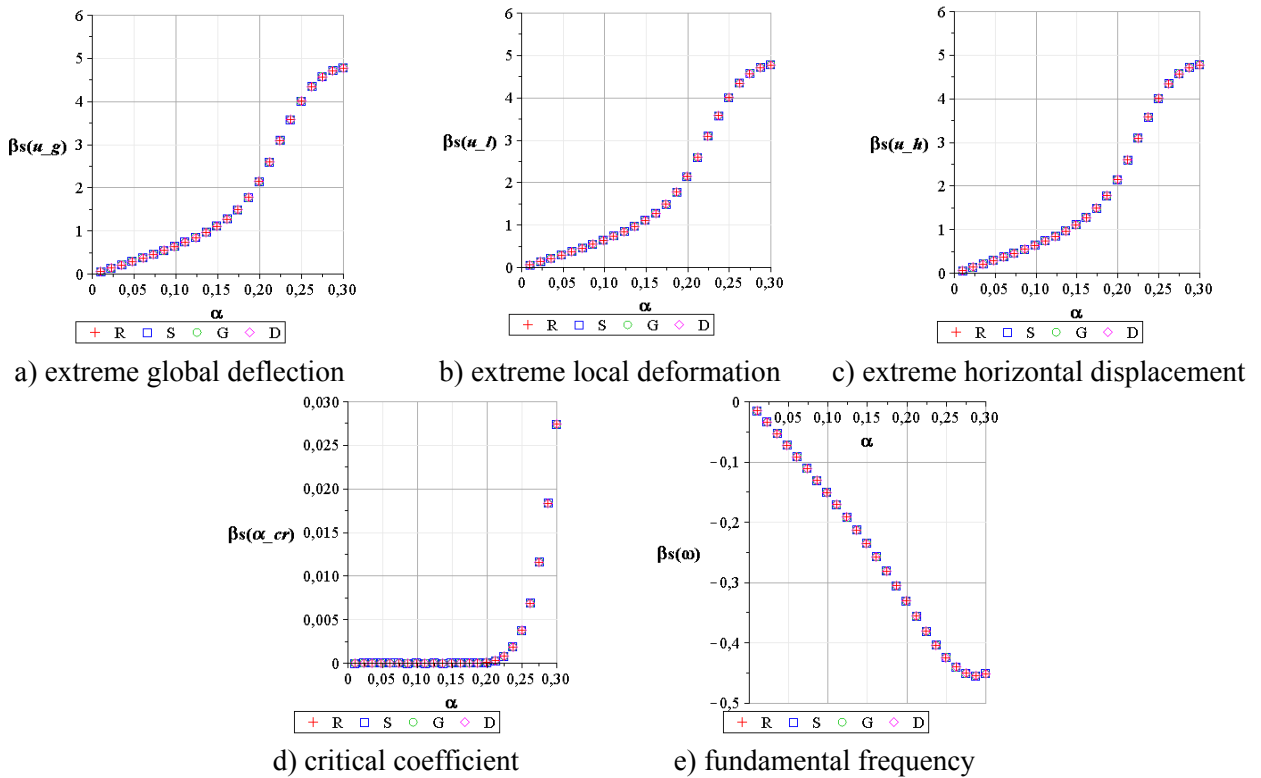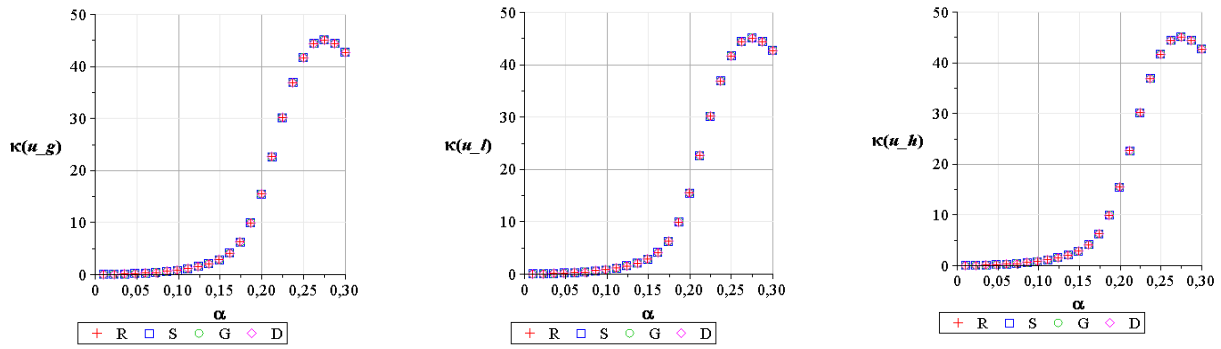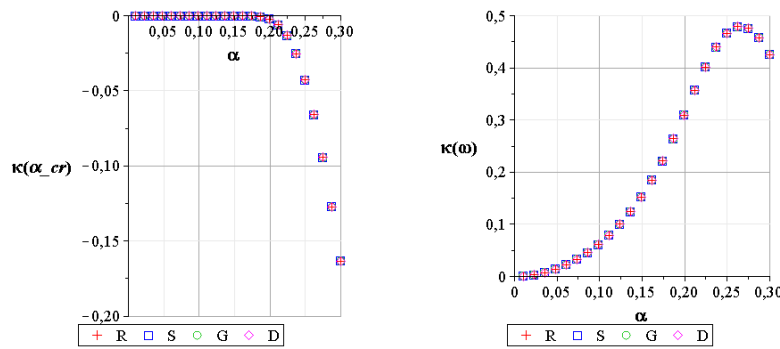
Fig.10. Variance for the analytical dependences.

a) extreme global deflection b) extreme local deformation c) extreme horizontal displacement

d) critical coefficient e) fundamental frequency
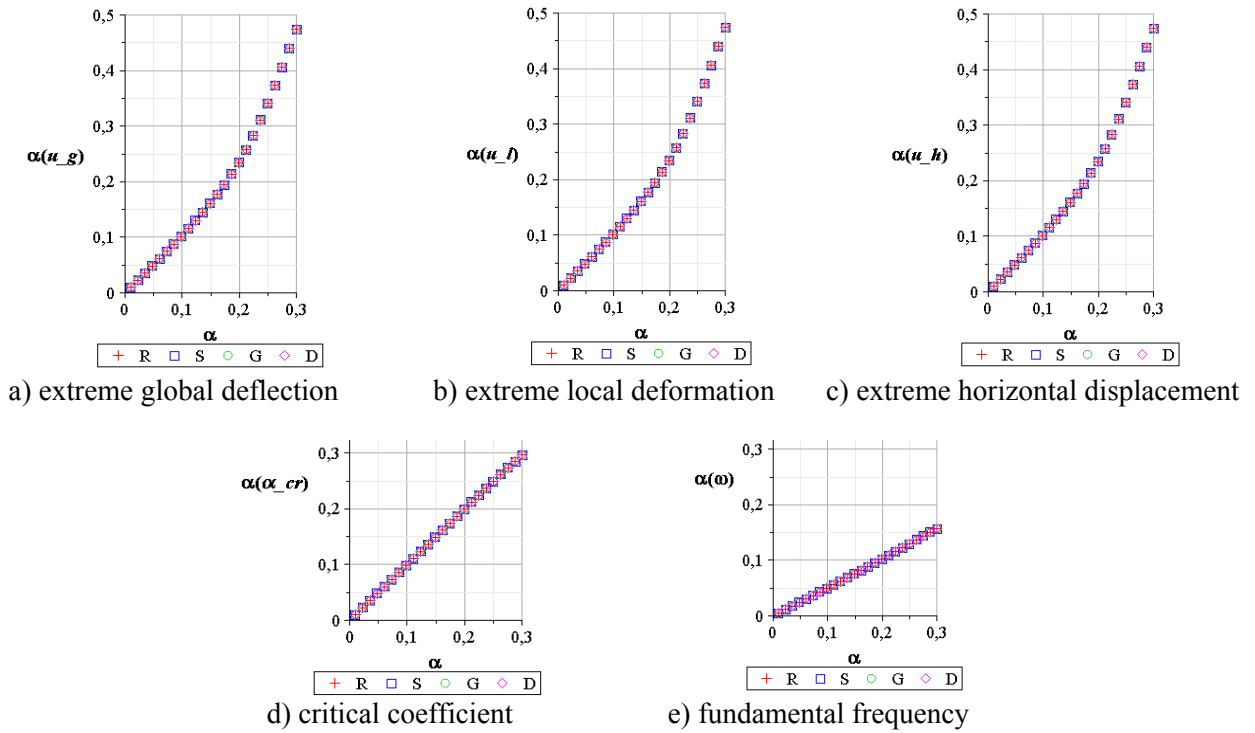
Fig.11. Coefficient of variation for the analytical dependences.

a) extreme global deflection b) extreme local deformation c) extreme horizontal displacement

d) critical coefficient e) fundamental frequency

Fig.12. Skewness for the analytical dependences.

a) extreme global deflection   b) extreme local deformation   c) extreme horizontal displacement

d) critical coefficient   e) fundamental frequency

Fig.13. Kurtosis for the analytical dependences.

Next, the Cornell reliability indices have been calculated by using the limit function g according to the following formula

$$\beta = \frac{E[g]}{\sqrt{\mathrm{Var}(b)}} = \frac{E[R-E]}{\sqrt{\mathrm{Var}(R-E)}} = \frac{E[R]-E[E]}{\sqrt{\mathrm{Var}(R)+\mathrm{Var}(E)}} \tag{5.1}$$

where *R* denotes the resistance, *E* stands for the effect of actions and the first two probabilistic moments have been determined by using Eqs (2.1)-(2.2). These reliability indices have also been computed by making the following assumptions: (1) the difference between frequency of forced vibration and fundamental frequency should be bigger than *25*%, (2) the limit for critical coefficient equals *1.0*, (3) the global vertical deflections are limited to *1/250* of the structure width (Eurocode 3-1-1, [19]), (4) the horizontal displacements should be smaller than *1/150* of the structure height (Eurocode 3-1-1, [19]) and (5) the limit for local deformation is specified as *1/500* of the element length (panels of toughened glass). Some of their variations upon the input coefficient of variation of the Young modulus (α) have been presented in Figs 14-15.

a) extreme global deflection   b) extreme local deformation   c) extreme horizontal displacement

d) critical coefficient   e) fundamental frequency
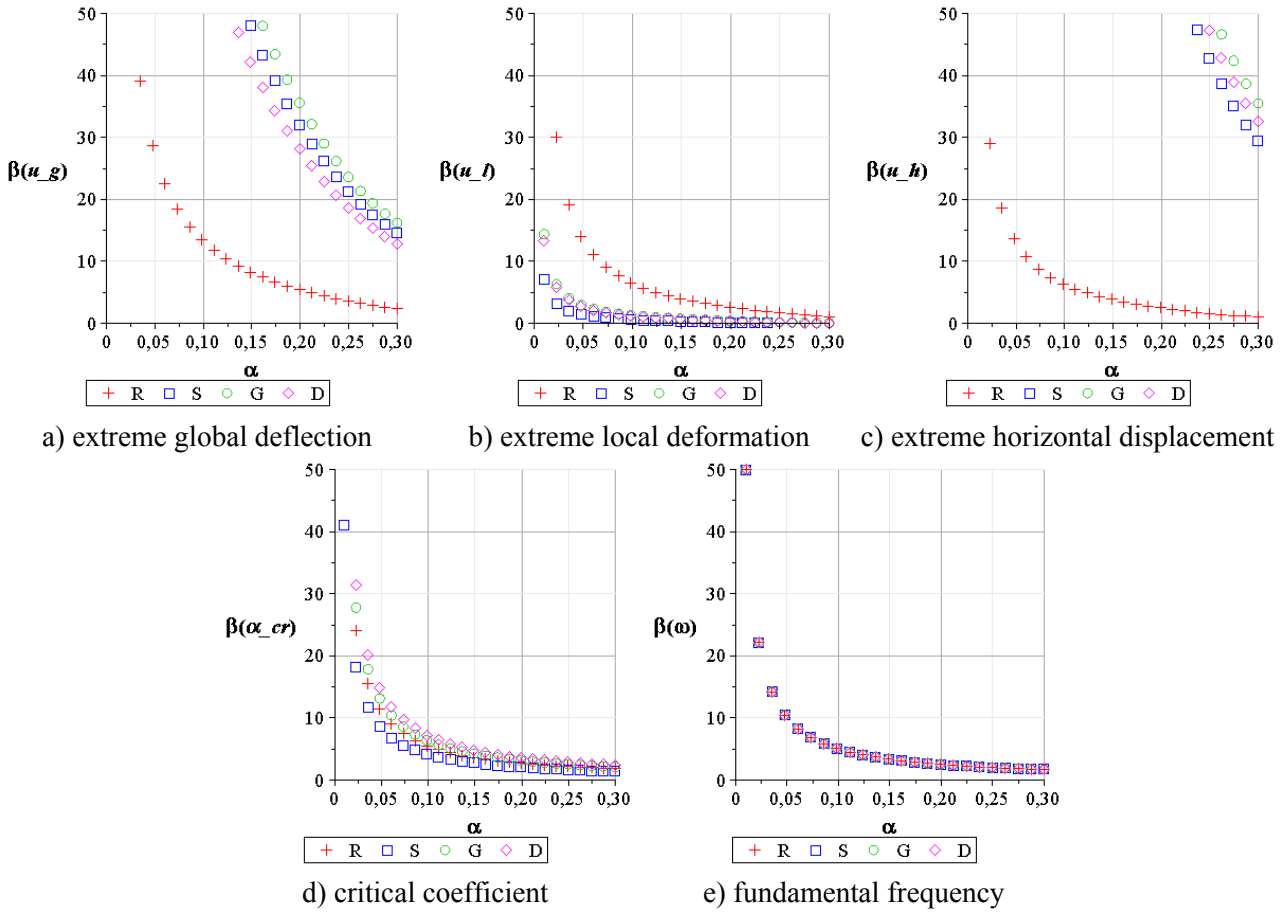
Fig.14. Reliability index of the given parameter for the analytical dependences.

All of them show that reliability indicators nonlinearly decrease together with an increase of uncertainty of the Young modulus, thereby the probability of failure increases, which is compliant with the engineering intuition in this matter. The final values are significantly sensitive to the coefficient α and even its small change results in the apparent change of these indices. The reliability indices concerning the fundamental frequency are almost identical for all domes (Fig.14e). For the first three parameters, the final values for Model R differ much from those obtained for the other models. In other cases, the reliability indices are similar (Figs 14a-d).

a) Model R   b) Model S   c) Model G   d) Model D
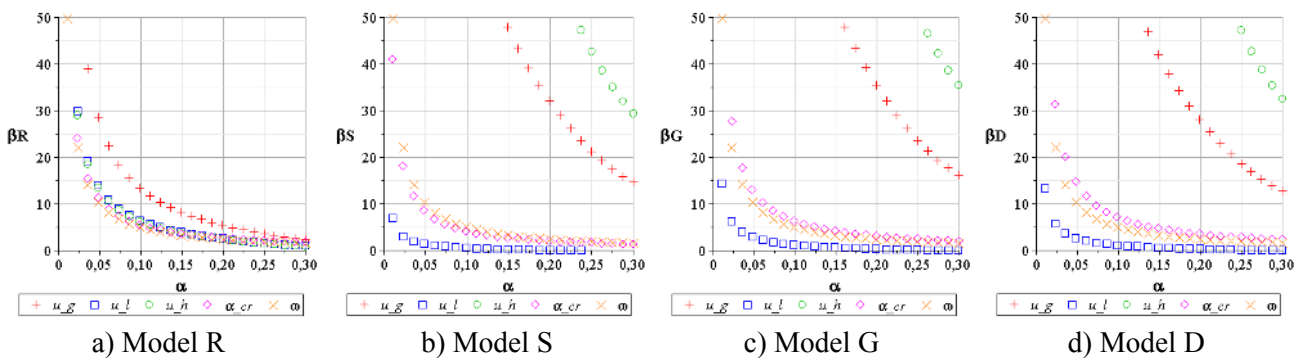
Fig.15. Reliability indices of the given model for the analytical dependences.

The minimal β values for Model R have been obtained for the fundamental frequency in the interval [*0.0,0.2*] and for the extreme horizontal displacement in the interval [*0.2,0.3*] (Fig.15a). For the remaining models, the indices for the local deflections are definitely smaller (Figs 15b-d). However, the β values should be further compared with their limits, which are lower for the Serviceability Limit State (Eurocode 0, [3]). The differences between the models were therefore examined by considering the minimum reliability index obtained for the first three parameters (Figs 14a-c). The results of this comparison are variable and depend on the SLS ratio, variance (Figs 10a-c) and input coefficient (Fig.16a). Nevertheless, the reliability index for Model R is the largest. The β value is initially by *78.2*% smaller for Model G, by *79.8*% for Model D and by *89.3*% for Model S (Fig.16a). However, masses, whose differences are significant, are not taken into account here.

a) without considering masses   b) considering masses
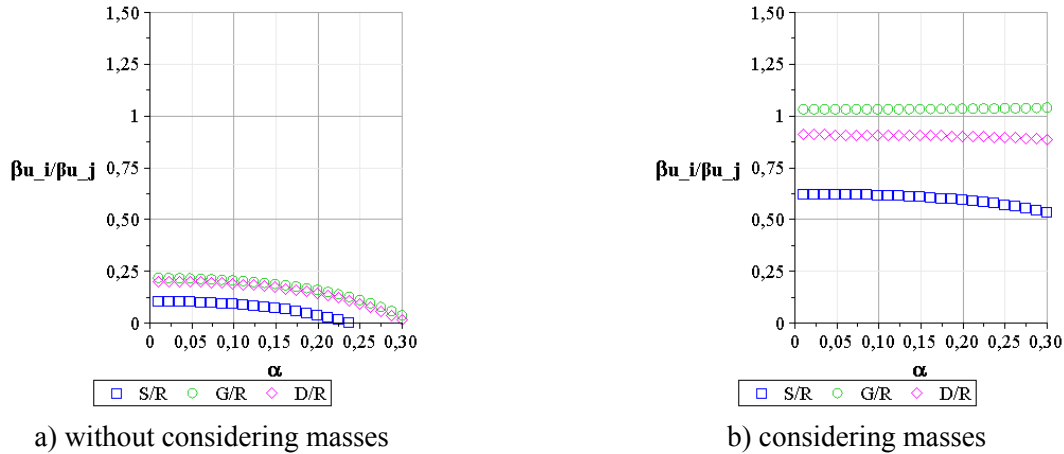
Fig.16. Ratio of the minimal reliability indices for the elastic displacements.

When we deal with response functions of the following form

$$f_i(b) = C_i \cdot g(b),\tag{5.2}$$

one can show that

$$E[E_i] = C_i \cdot I_1(a)\tag{5.3}$$

and

$$\mathrm{Var}(E_i) = C_i^2 \cdot I_2(a),\tag{5.4}$$

where C_i is a constant for the given model i, $g(b)$ is a function independent of the model choice, $I_1(a)$ and $I_2(a)$ are some integrals also independent on the model choice. Substitution of Eqs (5.3)-(5.4) into Eq.(5.1) and applying a simple as well as not very far-reaching assumption of inverse proportionality of stiffness to mass $(C_i = A_i / m_i)$ leads to the following formula for the given model

$$\beta_i = \frac{E[R_i] - E[E_i]}{\sqrt{\mathrm{Var}(R_i) + \mathrm{Var}(E_i)}} = \frac{E[R_i] - C_i \cdot I_1(a)}{\sqrt{0 + C_i^2 \cdot I_2(a)}} = \frac{E[R_i] - \dfrac{A_i}{m_i} \cdot I_1(a)}{\dfrac{A_i}{m_i} \cdot \sqrt{I_2(a)}}\tag{5.5}$$

where A_i is a constant for the given model i, and m_i is its mass. Further, let us define the mass normalized reliability index as

$$\overline{\beta_i} = \frac{E[R_i] - \frac{A_i}{m_0} \cdot I_1(a)}{\frac{A_i}{m_0} \cdot \sqrt{I_2(a)}} = \frac{E[R_i] - \frac{m_i}{m_0} \cdot C_i \cdot I_1(a)}{\frac{m_i}{m_0} \cdot C_i \cdot \sqrt{I_2(a)}} = \frac{E[R_i] - \frac{m_i}{m_0} \cdot E[E_i]}{\frac{m_i}{m_0} \cdot C_i \cdot \sqrt{I_2(a)}} \ . \tag{5.6}$$

Then, their ratio can be presented as follows

$$\frac{\overline{\beta_i}}{\beta_0} = \frac{E[R_i] - \frac{m_i}{m_0} \cdot E[E_i]}{\frac{m_i}{m_0} \cdot C_i \cdot \sqrt{I_2(a)}} \cdot \frac{\frac{m_0}{m_0} \cdot C_0 \cdot \sqrt{I_2(a)}}{E[R_0] - \frac{m_0}{m_0} \cdot E[E_0]} =$$

$$= \frac{E[R_i] - \frac{m_i}{m_0} \cdot E[E_i]}{E[R_0] - E[E_0]} \cdot \frac{C_0 \cdot m_0}{C_i \cdot m_i} = \frac{E[R_i] - \frac{m_i}{m_0} \cdot E[E_i]}{E[R_0] - E[E_0]} \cdot \frac{f_0(b^0) \cdot m_0}{f_i(b^0) \cdot m_i} \ . \tag{5.7}$$

The analytical dependence for elastic displacements – Eq.(3.1) – fulfils the condition given in Eq.(5.2), so masses have been taken into account during the reliability comparison for the models (Fig.16b). The differences between them significantly decreased and the geodesic dome turned out to be the most reliable of all the examined structures. Its final β value is initially by *3.3%* bigger than for Model R while for Model D is by *9.1%* smaller and for Model S – by *39.7%* (Fig.16b).

The influence of the analyzed response functions on the results has been compared numerically, not visually, due to their very large number (several thousand). The maximum value of the input coefficient of variation has been sought for which the results would be close to those obtained from the analytical method. This value is hereinafter called the relevance interval coefficient (*RIC*). Simultaneous exceeding of the one-percent relative and absolute error has been assumed as the stop criterion. For large values, the relative error has been decisive, while for small ones (smaller than *1*) - absolute.

The relevance interval coefficient depends on:
− the model (index - d),
− the parameter (index - p),
− the given probability-based coefficient: the expectation, the variance, the output coefficient of variation, the skewness, the kurtosis or the reliability index (index - m),
− the order of base function,
− the number of trial points,
− and the way the response function is created.

If some *RIC* coefficient being the minimum from the above categories is considered, the corresponding index is added to shorten notation. For example, the RIC_{dp} value is calculated as the minimum from all models and parameters. The index d and m have always been used so that the response function would describe all the different domes equally well and the accidental relevance only for the reliability index would be avoided

The results of the first part of the analysis show that the optimal functions computed using the Rational Interpolation, as expected, perfectly approximate dependences for the elastic displacements (Figs 17a-c) and the critical coefficient (Fig.17d) already for *N = 11*. More points are required to obtain maximum correctness in the case of the first eigenfrequency (Fig.17e). However, all criteria (K, V and M) ideally indicate the optimal functions generated.

The Least Squares Method, as well as its weighted version, provide satisfactory relevance only for the critical coefficient (Fig.17d), which is quite obvious. Therefore, it is pointless to consider the criterion for choosing the optimal polynomial. It is worth noting, however, that the WLSM results are never better than those obtained from the LSM (Figs 17a-e).
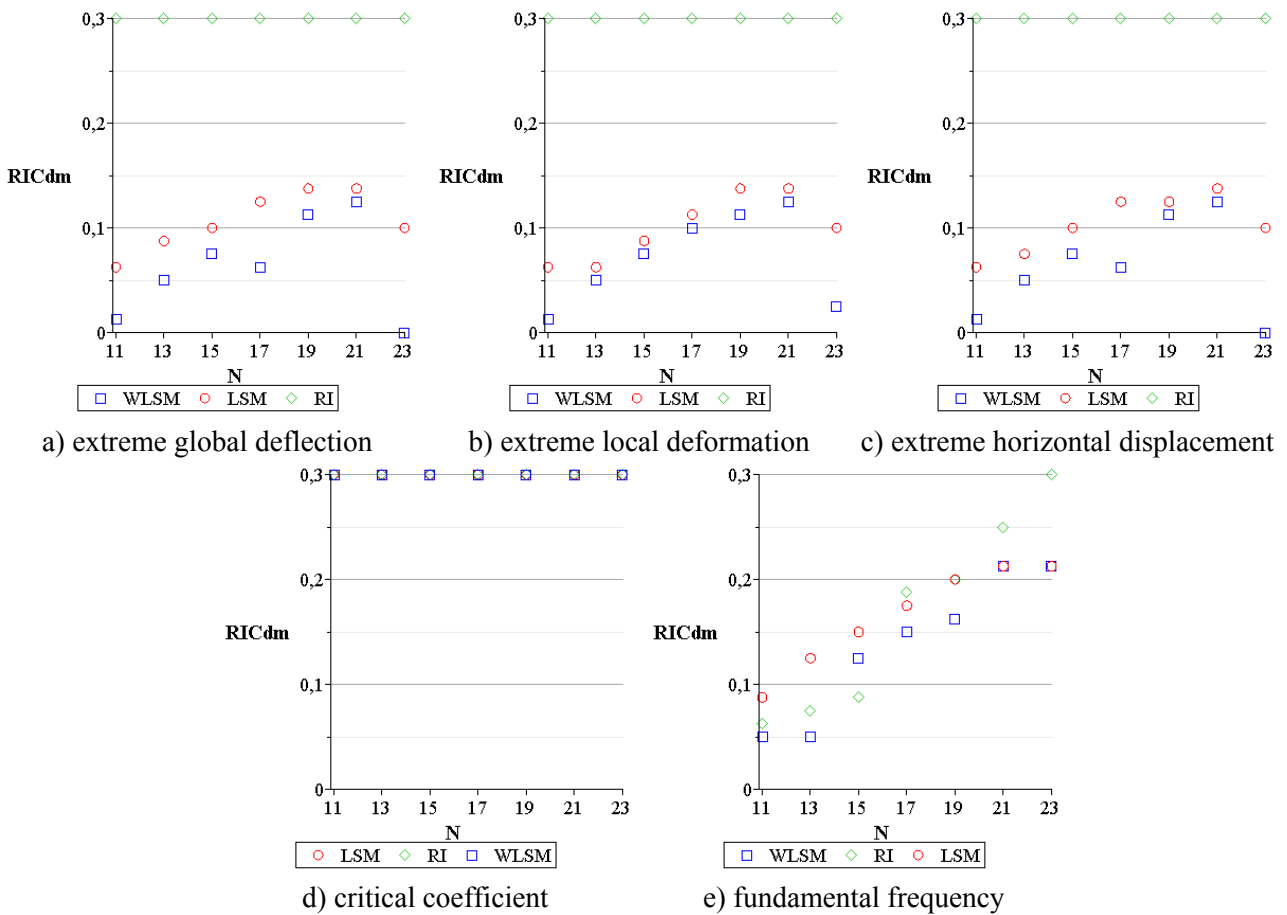
a) extreme global deflection   b) extreme local deformation   c) extreme horizontal displacement

d) critical coefficient   e) fundamental frequency

Fig.17. Minimal *RIC* coefficient of all models and probability-based coefficients for the given parameter and the optimal function for the given method.

The choice of the method should be made in order to obtain satisfactory relevance for all parameters. Only the results of the RI method (Fig.18) meet these requirements, but for a higher than normal number of trial points. At the same time, the selection of the optimal function from all methods based on each criterion (K, V, M) always indicates the Least Squares Method.
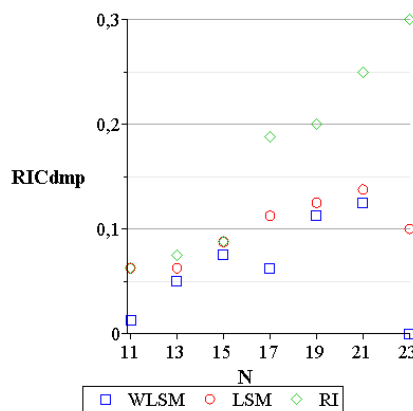
Fig.18. Minimal *RIC* coefficient of all models, parameters and probability-based coefficients for the optimal function for the given method.

The results from Fig.18 coincide with an engineering intuition in this matter. As the number of points increases, the width of the interval in which the function values are correct also increases. Therefore, the integration with more and more values of the input coefficient of variation gives the relevant value. However, when switching from *N = 21* to *N = 23*, the WLSM and LSM results unexpectedly fall. Polynomials up to the tenth order turn out to be insufficient to correctly approximate such a large number of trial points (Fig.19). These two additional points are also far removed from the others (Tab.1).

a) *N = 21*   b) *N = 23*
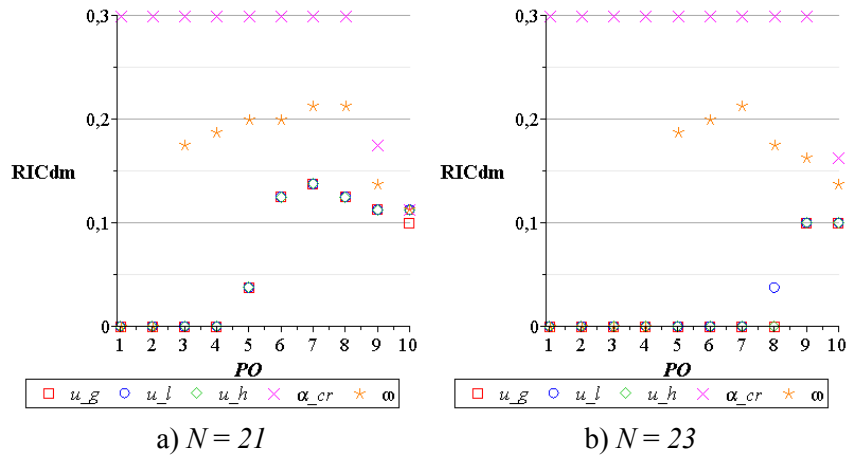
Fig.19. Minimal *RIC* coefficient of all models and probability-based coefficients for the given *N*.

Obtaining FEM results in a wide range may not always be possible, and most importantly requires a large amount of time. Therefore, in the second part of the analysis, generalizations of the most frequently used empirical formulas have been tested (Tab.2) to increase the correctness of LSM approximation already for *N = 11*.

The given function group used for all parameters does not lead to satisfactory relevance. Choosing the response functions from all groups has turned out to be a much better solution (Fig.20). The criteria K1, K2, M1 and M2 perfectly approximate dependences for all parameters. However, the dependence of the *RIC* coefficient on the criterion value is most apparent for M1. This situation occurs for both optimal functions (Fig.21) and for all generated functions in the groups (Fig.22).
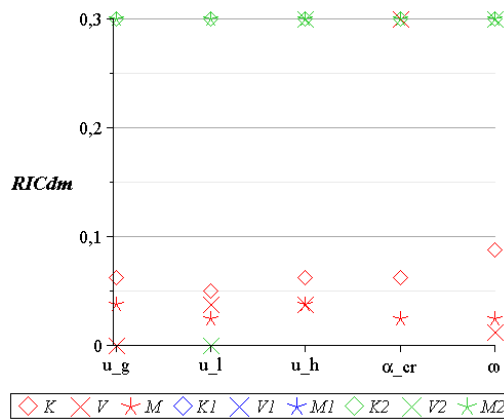

Fig.20. Minimal *RIC* coefficient of all models and probability-based coefficients for the given criterion of response function choosing.

The values of the criterion M1, above which full relevance was obtained, differ depending on the parameter (Figs 21-22). The maximum (for the fundamental frequency) can be rounded up to 10^{22}, which is approximately *1/100* of the minimum value obtained for the analytical dependences (Fig.21). The final results of this part of the analysis are collected in Tab.6.
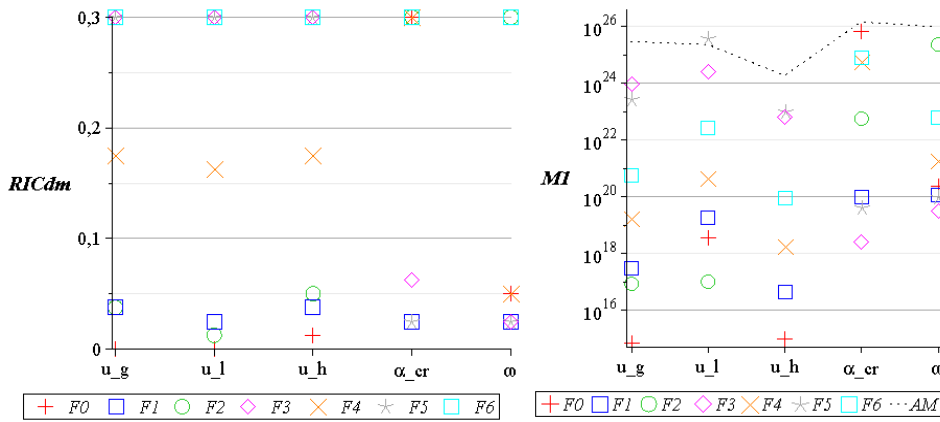

Fig.21. RIC_{dm} coefficient and *M1* criterion values for the optimal response function from the given group (Least Squares Method, *N = 11*).

a) extreme global deflection b) extreme local deformation c) extreme horizontal displacement

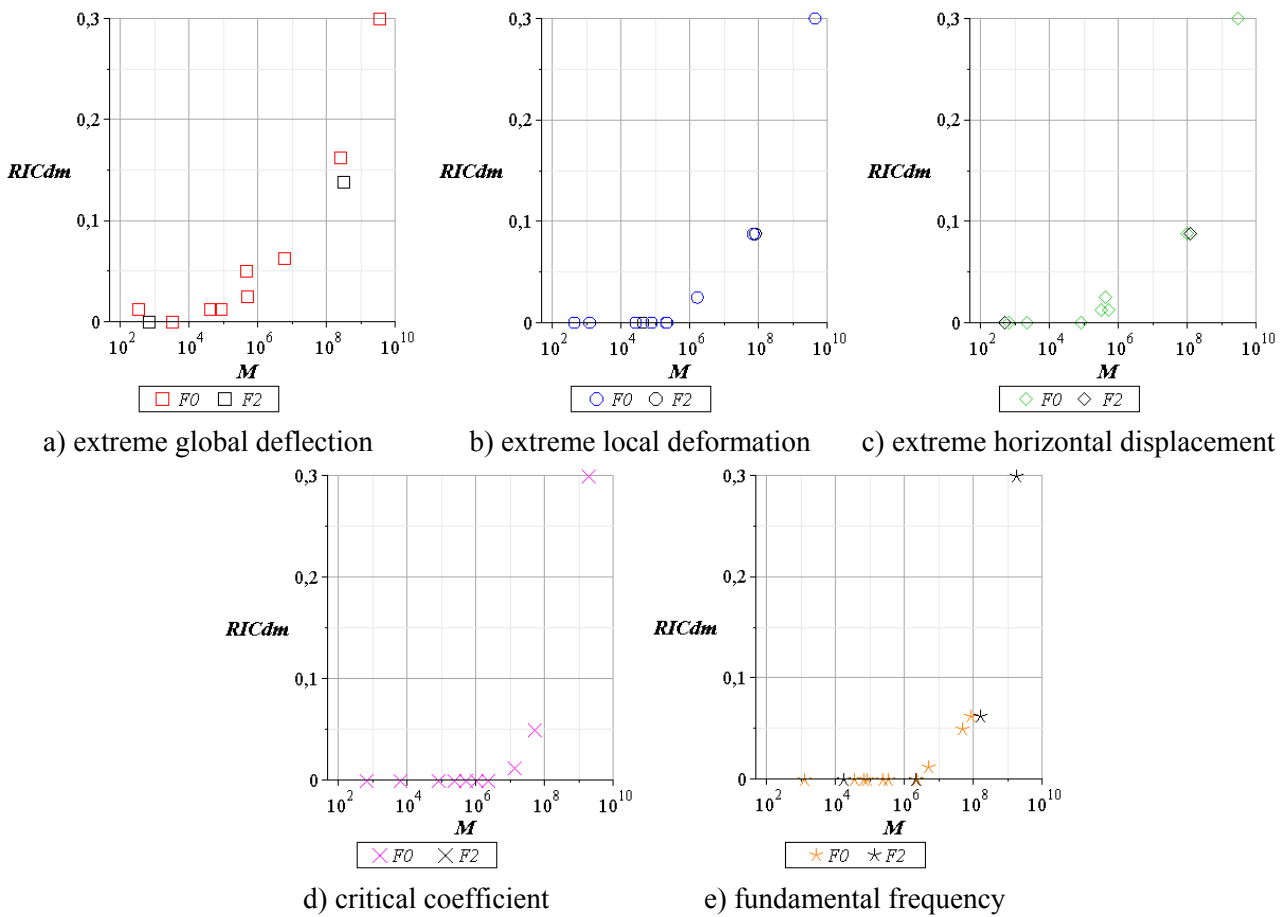d) critical coefficient e) fundamental frequency
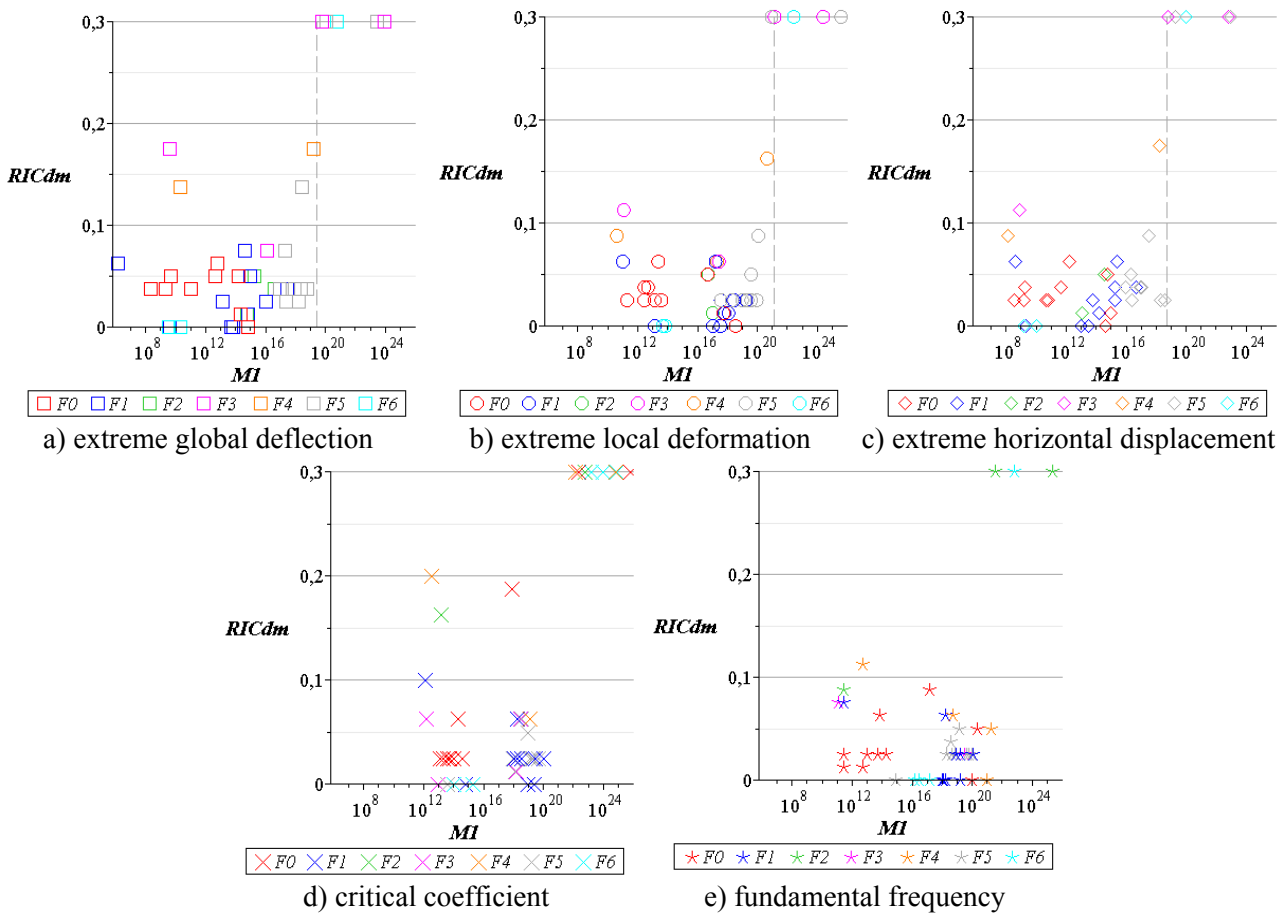
Fig.22. Minimal *RIC* coefficient of all models and probability-based coefficients for the given parameter and various functions from the given group (Least Squares Method, *N = 11*).

Table 6. Comparison of the analytical dependences results with those obtained for optimal response functions from the groups.

parameter	analytical dependences		optimal responses from the groups	
	formula	M1 criterion value	formula	M1 criterion value
u_g	$\dfrac{C}{b}$	$2.76 \cdot 10^{25}$	$\dfrac{1}{C \cdot b + D}$	$9.29 \cdot 10^{23}$
u_l	$\dfrac{C}{b}$	$2.22 \cdot 10^{25}$	$\dfrac{C}{b} + D$	$3.90 \cdot 10^{25}$
u_h	$\dfrac{C}{b}$	$1.84 \cdot 10^{24}$	$\dfrac{C}{b} + D$	$9.80 \cdot 10^{22}$
α_cr	$C \cdot b$	$1.38 \cdot 10^{26}$	$C \cdot b + D$	$6.48 \cdot 10^{25}$
ω	$C \cdot \sqrt{b}$	$9.58 \cdot 10^{25}$	$\sqrt{C \cdot b + D}$	$2.35 \cdot 10^{25}$

a) extreme global deflection   b) extreme local deformation   c) extreme horizontal displacement

d) critical coefficient   e) fundamental frequency

Fig.23. Minimal *RIC* coefficient of all models and probability-based coefficients for the given parameter and various functions from the given group (Rational Interpolation, $N = 11$).

In the case of the Rational Interpolation method only for the fundamental frequency, the approximation is not fully correct for $N = 11$ (Fig.17e). However, the dependence of the *RIC* coefficient

on the M criterion value is always clearly apparent (Figs 23a-e). This situation occurs for all generated rational functions. The values of the criterion M, above which full relevance was obtained, can be rounded up for all parameters to 10^9. In the case of approximation of the fundamental frequency with rational functions ($N = 11$), the result was $8.41 \cdot 10^7$, which explains the lack of full relevance. The application of the formula from the F2 group (Tab.2) was enough to obtain the value of the criterion M equal to $1.76 \cdot 10^9$, and thus the full correctness (Fig.23e).

The above-mentioned methods of improving the relevance interval for $N = 11$ have been used to approximate the displacements obtained from the second-order global analysis P-Delta. In the case of the RI method, the largest value of criterion M was $3.05 \cdot 10^7$ and further searching for the responses would be necessary. Fortunately, the LSM method has achieved satisfactory values of the M1 criteria. They are presented in Figs 22a-c as vertical dashed lines. The optimal responses have the following form for Model G

$$u\_g_G = -1.67990 \cdot 10^{-2} + \frac{3.53369 \cdot 10^3}{b} + \frac{1.95765 \cdot 10^4}{b^2} + \frac{6.54447 \cdot 10^5}{b^3} \,, \tag{5.8}$$

$$u\_l_G = -1.50535 \cdot 10^{-3} + \frac{1.21019 \cdot 10^3}{b} - \frac{2.13714 \cdot 10^3}{b^2} \,, \tag{5.9}$$

$$u\_h_G = -1.41970 \cdot 10^{-3} + \frac{1.40861 \cdot 10^3}{b} + \frac{3.97371 \cdot 10^3}{b^2} + \frac{4.51853 \cdot 10^4}{b^3} \,. \tag{5.10}$$

The values of the reliability indices obtained in this way (Figs 24a-c) are of course smaller than those for elastic displacements (Figs 14a-c). This time, the minimal β values for Model R have been obtained for the horizontal displacements in the entire considered interval (Fig.25a). For the remaining models, the indices for the local deflections are still definitely smaller (Figs 25b-d). Therefore, the reliability indices for the displacements are the ones, which decides about the fulfilment of the condition of reliability.
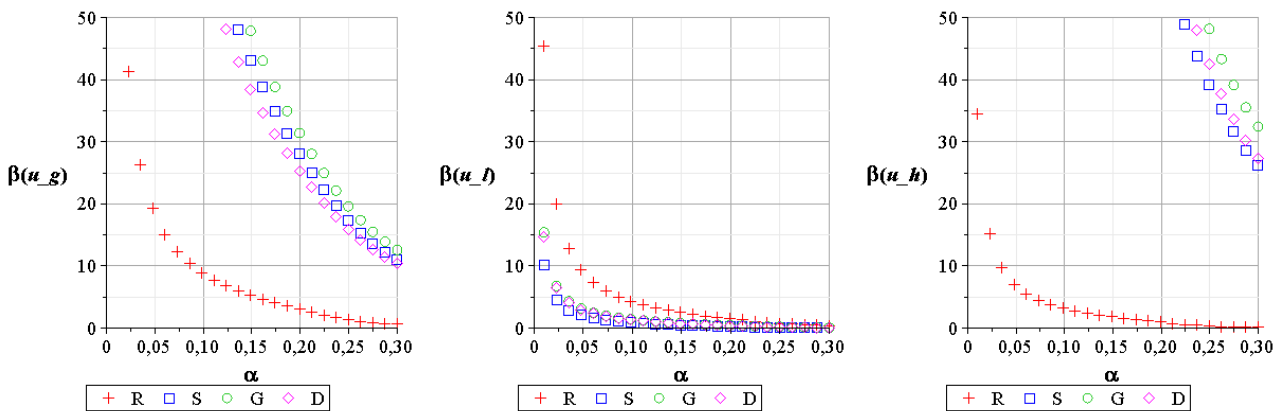
a) extreme global deflection   b) extreme local deformation   c) extreme horizontal displacement

Fig.24. Reliability index of the given parameter for the second-order analysis results.

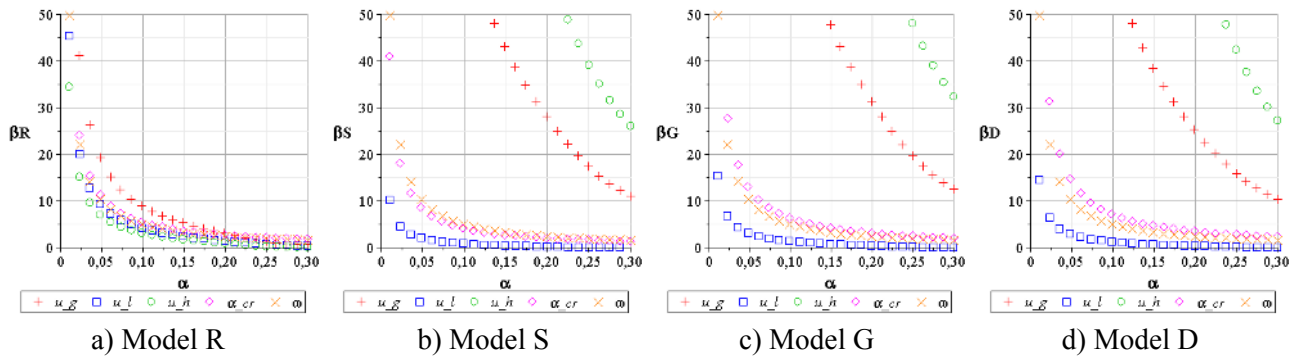a) Model R   b) Model S   c) Model G   d) Model D

Fig.25. Reliability indices of the given model for the displacements obtained for the second-order analysis results.

Without considering masses, the reliability index for Model R is still the biggest. The β value is initially by *55.4*% smaller for Model G, by *57.6*% for Model D and by *70.5*% for Model S (Fig.26a). The differences are therefore clearly smaller than when considering elastic displacements (Fig.16a).
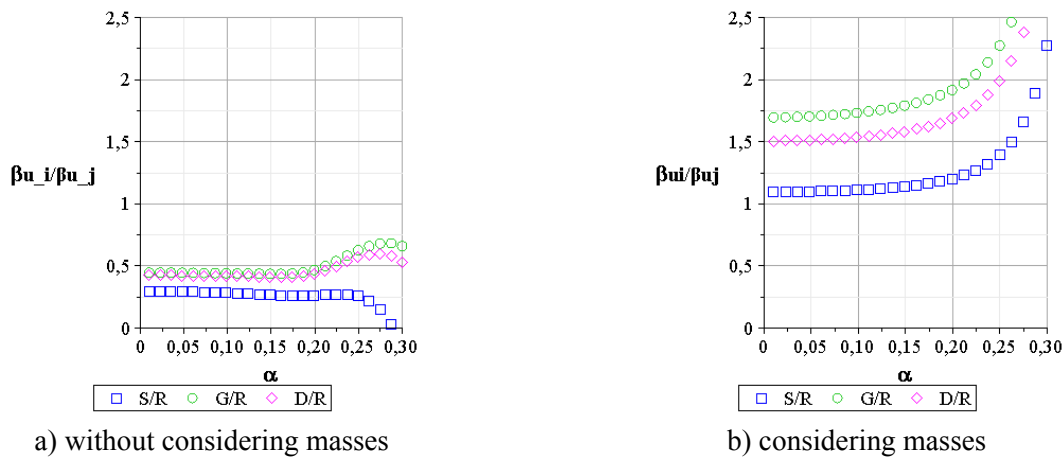

a) without considering masses   b) considering masses

Fig.26. Ratio of the minimal reliability indices for the displacements in the second-order analysis P-Delta.

Unfortunately, the functions describing the results of the second-order analysis do not fulfil the condition given in Eq.(5.2). However, Eq.(5.7) have been used to at least take into account the influence of the mass during the reliability comparison for the models. The geodesic dome again has proved to be the most reliable of all the examined structures (Fig.26b).

6. Concluding remarks

The most important research finding in this work is that the analyzed response functions have a meaningful influence on the probabilistic moments and coefficients. The maximum value of the input coefficient of variation for which the results are close to those obtained from the analytical method has been called the relevance interval coefficient (RIC). It is confirmed directly by the computations that as the number of trial points goes up, the value of this coefficient increases. It perfectly coincides with an engineering intuition in this matter. However, the polynomials order should be high enough to sufficiently approximate a large number of trial points. Rational functions have proved to be relevant in the widest interval of α here (Fig.18). At the same time, polynomials computed using the LSM method have turned out to be better approximation than those obtained from the WLSM method.

Determination of the FEM results in a wide range of design input parameter variability may not always be available, and most importantly requires a large amount of time. Therefore, some generalizations of the most frequently used empirical formulas (Tab.2) have been proposed to increase efficiency of such an approximation just for $N = 11$ trial tests. There have been noted two apparent dependences of the *RIC* coefficient on the criterion value of the FEM experiments series with the proposed fitting. Its rounded up maximum, above which full relevance was obtained, equals 10^{22} for the criterion M1 in the LSM and 10^9 for the criterion M in the Rational Interpolation. If the structural response is unavailable, it is suggested to look for an approximation that meets one of these conditions. Both methods have their advantages and disadvantages.

Computational analysis provided in this paper shows also that the reliability index for the ribbed dome is remarkably the biggest without considering masses (Figs 16a and 26a). However, the difference between them is significant, so the way of taking masses into account has been proposed. The geodesic dome has turned out then to be the most effective (from the examined structures) in terms of reliability with the Young modulus as input random variable. Already for the first-order analysis, its mass normalized reliability index is the highest. According to the results of the second order analysis, it should be even better, particularly since the difference in reliability indices that do not take into account the mass is lower.

The direct symbolic integration approach presented in this paper is an accurate tool to verify the influence of the response functions choice as well as to determine the values of the reliability indices for different performance functions. It needs, however, an additional computer algebra program and the response functions that are integrable together with a given probability density function. It is confirmed directly by the computations that with an increase of uncertainty in the Young modulus, the reliability indices of the domes analyzed always decrease. It perfectly coincides with an engineering intuition in this matter.

The values of reliability index β for different limit states can be further used in reliability assessment by comparing the minimal one (connected in this case with the extreme horizontal displacements or local deformations) with its limit dependent upon the reliability class, a reference period and a type of the given limit state given in the Eurocode [3].

Nomenclature

A, C, D — constants

b — stationary input random variable

$2\Delta b$ — computational domain range

E — effect of actions

$E\big[f(b)\big]$ — expectation of the function $f(b)$, Eq.(2.1)

$f_i(b)$ — some real function for a given model, Eq.(5.2)

g — limit function

$g(b)$ — function independent on the model choice

$I_1(\alpha), I_2(\alpha)$ — integrals independent on the model choice

m — mass

N — trial points number

$p_b(x)$ — probability density function of the variable b, Eq.(2.7)

R — resistance

RIC — relevance interval coefficient

$u(b)/v(b)$ — approximation in the Rational Interpolation

u_g — extreme global deflection

u_h — extreme horizontal displacement

u_l — extreme local deformation

$\text{Var}\big(f(b)\big)$ — variance of the function $f(b)$, Eq.(2.2)

$w(b)$ — response function approximation in the Least Squares Method

α — input coefficient of variation

α_cr — critical coefficient

$\alpha(f(b))$ — coefficient of variation of the function $f(b)$, Eq.(2.4)

β — reliability index, Eq.(5.1)

$\bar{\beta}$ — mass normalized reliability index, Eq.(5.6)

$\beta_s(f(b))$ — skewness of the function $f(b)$, Eq.(2.5)

$\kappa(f(b))$ — kurtosis of the function $f(b)$, Eq.(2.6)

μ — effective length coefficient

$\mu_m(f(b))$ — mth central probabilistic moment of the function $f(b)$, Eq.(2.3)

$\sigma(b)$ — standard deviation of the variable b

ω — fundamental frequency

$(.)^0$ — mean value of the parameter $(.)$

Subscripts

i — designation of a given model

m — order of central probabilistic moment

References

[1] Lan T. (1999): *Space Frame Structures*. In Chen W.-F. & Lui E. (Eds.), Handbook of Structural Engineering (2nd ed.) – CRC Press, Boca Raton.

[2] Szaniec W. and Biernacka K. (2013): *Modal Analysis of Selected Bar Domes.* – Structure and Environment, Kielce – vol.5, No.4, pp.15-20.

[3] The European Union Regulation (2002a): *Eurocode: Basis of structural design*.

[4] Pokusiński B. and Kamiński M. (2018): *On influence of the response functions on the diagrid and orthogonal grillages reliability by the stochastic iterative perturbation-based finite element method* – Proceedings of the 22nd International Conference on Computer Methods in Mechanics, Lublin – vol.1922, No.150011, pp.1-10.

[5] Kamiński M. and Szafran J. (2009): *Random eigenvibrations of elastic structures by the response function method and the generalized stochastic perturbation technique* – Archives of Civil & Mechanical Engineering, Wrocław – vol.9, No.4, pp.5–32.

[6] Solecka M., Kamiński M. and Szafran J. (2011): *Comparison of the aluminium versus steel telecommunication towers in Stochastic Finite Element Method eigenvibrations analysis* – Int. J. Mechanics and Mechanical Engineering, Łódź – vol.15, No.1, pp.95–110.

[7] Kamiński M. (2013): *The stochastic perturbation method for computational mechanics* – Wiley, Chichester.

[8] Kottegoda K. and Rosso R. (2008): *Applied statistics for civil and environmental engineers* – Blackwell, Chichester.

[9] Murzewski J. (1989): *Reliability of engineering structures* [in Polish] – Warsaw: Arkady.

[10] Kamiński M. and Szafran J. (2015): *Least Squares Stochastic Finite Element Method in structural stability analysis of steel skeletal structures* – International Journal of. Applied Mechanics and Engineering, Zielona Góra – vol.20, No.2, pp.299–318.

[11] Kamiński M. and Świta P. (2009): *Numerical simulation of the Euler problem for the elastic beams with random parameters* – Proc. IASS Local Polish Seminar, Warsaw – pp.74-82.

[12] Kamiński M. and Świta P. (2011): *Reliability modeling in some elastic stability problems via the Generalized Stochastic Finite Element Method* – Archives of Civil Engineering, Warsaw – vol.57, No.3, pp.275-295.

[13] Beckermann B. and Labahn G. (2000a): *Fraction-free computation of matrix rational interpolants and matrix GCDs.* – SIAM Journal on Matrix Analysis and Applications, Philadelphia – vol.22, No.1, pp.114-144.

[14] Beckermann B. and Labahn G. (2000b): *Numeric and symbolic computation of problems defined by structured linear systems* – Reliable Computing – vol.6, No.4, pp.365-390.

[15] Bronsztejn I., Siemiendiajew K., Musiol G. and Muhlig H. (2009): *Modern compendium of mathematics* [in Polish] – Warsaw: Wydawnictwo Naukowe PWN.

[16] The European Union Regulation (2003): *Eurocode 1: Actions on structures – Part 1-3: General actions - Snow loads*.

[17] The European Union Regulation (2005): *Eurocode 1: Actions on structures – Part 1-4: General actions - Wind actions*.

[18] The European Union Regulation (2002b): *Eurocode 1: Actions on structures – Part 1-1: General actions - densities, self-weight, imposed loads for buildings*.

[19] The European Union Regulation (2006): *Eurocode 3: Design of steel structures – Part 1-1: General rules and rules for buildings*.